0254-6124/2016/36(3)245—22 *Chin. J. Space Sci.* 空间科学学报

XIONG Ming, LIU Ying, LIU Hao, LI Baoquan, ZHENG Jianhua, ZHANG Cheng, XIA Lidong, ZHANG Hongxin, RAO Wei, CHEN Changya, SUN Weiying, WU Xia, DENG Yuanyong, HE Han, JIANG Bo, WANG Yuming, WANG Chuanbing, SHEN Chenglong, ZHANG Haiying, ZHANG Shenyi, YANG Xuan, SANG Peng, WU Ji. Overview of the Solar Polar Orbit Telescope project for space weather mission. *Chin. J. Space Sci.*, 2016, **36**(3): 245-266. DOI:10.11728/cjss2016.03.245

Overview of the Solar Polar Orbit Telescope Project for Space Weather Mission*

XIONG Ming[1] LIU Ying[1] LIU Hao[1] LI Baoquan[1] ZHENG Jianhua[1]

ZHANG Cheng[1] XIA Lidong[2] ZHANG Hongxin[3] RAO Wei[4] CHEN Changya[5]

SUN Weiying[1] WU Xia[1] DENG Yuanyong[6] HE Han[6] JIANG Bo[7]

WANG Yuming[8] WANG Chuanbing[8] SHEN Chenglong[8] ZHANG Haiying[9]

ZHANG Shenyi[1] YANG Xuan[1] SANG Peng[1] WU Ji[1]

1(*National Space Science Center, Chinese Academy of Sciences, Beijing* 100190)

2(*Center for Space Weather Sciences, Shandong University at Weihai, Weihai* 264200)

3(*Changchun Institute of Optics, Fine Mechanics and Physics, Chinese Academy of Sciences, Changchun* 130033)

4(*Beijing Institute of Spacecraft System Engineering, China Aerospace Science and Technology Corporation, Beijing* 100094)

5(*Shanghai Institute of Satellite Engineering, China Aerospace Science and Technology Corporation, Shanghai* 200030)

6(*National Astronomical Observatories, Chinese Academy of Sciences, Beijing* 100012)

7(*Xi'an Institute of Optics and Precision Mechanics, Chinese Academy of Sciences, Xi'an* 710119)

8(*School of Earth and Space Sciences, University of Science and Technology of China, Hefei* 230026)

9(*Nanjing Institute of Astronomical Optics and Technology, Chinese Academy of Sciences, Nanjing* 210042)

Abstract The Solar Polar ORbit Telescope (SPORT) project for space weather mission has been under intensive scientific and engineering background studies since it was incorporated into the Chinese Space Science Strategic Pioneer Project in 2011. SPORT is designed to carry a suite of remote-sensing and in-situ instruments to observe Coronal Mass Ejections (CMEs), energetic particles, solar high-latitude magnetism, and the fast solar wind from a polar orbit around the Sun. The first extended view of the polar regions of the Sun and the ecliptic enabled by SPORT will provide a unique opportunity to study CME propagation through the inner heliosphere, and the solar high-latitude magnetism giving rise to eruptions and the fast solar wind. Coordinated observations between SPORT and other spaceborne/ground-based facilities within the International Living With a Star (ILWS) framework can significantly enhance scientific output. SPORT is now competing for

* Supported by the Strategic Priority Research Program on Space Science (XDA04060801, XDA04060802, XDA04060803, XDA04060804) of Chinese Academy of Sciences, the Specialized Research Fund for State Key Laboratory of China, the Chinese National Science Foundation (41374175, 41204129), and the CAS/SAFEA international Partnership Program for Creative Research Teams

Received February 21

E-mail: mxiong@spaceweather.ac.cn

official selection and implementation during China's 13th Five-Year Plan period of 2016—2020.

Key words Space weather, Coronal mass ejection, Solar magnetism, Solar wind, Solar energetic particle

Classified index P 35

0 Introduction

The heliosphere represents a uniquely accessible domain to study fundamental physical processes common to space and laboratory plasmas that cannot be studied from astronomical distances or reproduced on Earth. Understanding the causal connections between the Sun and the heliosphere is of fundamental importance to space physics and space weather[1−2]. The Sun, interplanetary space, and Earth can be viewed as key elements of an interconnected system. The inner heliosphere is permeated with the supersonic and magnetized solar wind from the Sun. The solar wind consists of dominant protons and electrons as well as minor heavy ions. The solar wind plasma is collisionless, and waves/turbulence are ubiquitous[3−6]. The solar wind is the only available plasma "laboratory" where turbulence can be studied without interference from spatial boundaries and in the important domain of very large magnetic Reynolds numbers.

Coronal Mass Ejections (CMEs), carrying large-scale expulsions of plasma and magnetic field from the corona, frequently disturb the background solar wind flow[7−9]. The source regions of CMEs on the photosphere usually have highly-sheared magnetic field lines. A sudden disruption of the complex magnetic configuration leads to a large-scale expulsion of plasma and magnetic field from the corona. Such a catastrophic process typically develops in the low corona within 10∼15 minutes. CMEs can accelerate rapidly during the early stages of their formation and reach speeds of up to 3000 $\mathrm{km\cdot s^{-1}}$. As a result, the accelerated, heated, and magnetized CMEs generally carry a total energy of 10^{32} erg into interplanetary space. CMEs are the main driver of interplanetary and geomagnetic disturbances[10−11]. Multiple CMEs moving at different speeds collide and merge, smoothing out the flow and removing information about their relative origins[12−18]. CMEs are also the main driver of hazardous space weather effects[19]: (i) CMEs are often associated with a sustained southward magnetic field, which allows a strong coupling between the solar wind and the magnetosphere; (ii) CMEs can generate interplanetary shocks, a key source of energetic particles and radio bursts. CMEs may also be of astrophysical interest since they may be the dominant way that stars shed both magnetic flux and magnetic helicity that are built up as a result of the stellar dynamo[20−21].

An international effort to understand the heliosphere and its space weather transients should be taken with a fleet of spacecraft carrying remote-sensing observations at visible, Extreme Ultra-Violet (EUV), and X-ray wavelengths, as well as in-situ measurements of interplanetary plasmas, particles, and fields. Coordinated remote-sensing and in-situ observations can track the propagation, evolution, and possible interactions of CMEs. Stereoscopic white-light imaging of a large portion of the inner heliosphere is successfully realized by the twin Solar TErrestrial RElations Observatory (STEREO) spacecrafts within the ecliptic[22−24], but still unavailable from viewpoints of polar orbits. The injection of the spacecraft to a solar polar orbit is difficult. Tremendous energy is needed for a spacecraft to escape from the ecliptic, so the gravity assist from Jupiter is necessary to bend the flight path of the spacecraft. As an out-of-ecliptic mission, the International Solar Polar Mission (ISPM) was thereby proposed in the 1970s[25]. For the ISPM, two spacecrafts were to be built by National Aeronautics and Space Adminis-

tration (NASA) and European Space Agency (ESA), respectively. One would be sent over Jupiter, then under the Sun. The other would fly under Jupiter, then over the Sun. All solar imaging instruments of the ISPM were to be accommodated on the NASA spacecraft. However, due to cutbacks, the NASA spacecraft was canceled in 1981. For the remaining ESA spacecraft, NASA provided a Radioisotope Thermoelectric Generator (RTG) and the launch services. Then, the ISPM was recast as Ulysses, due to the indirect and untried flight path. Ulysses was first launched with a space shuttle in 1990, then swung by Jupiter, and finally reached an inclination of 80°. Till now, Ulysses is the sole out-of-ecliptic mission to orbit the Sun and study the solar wind at all latitudes[26−29].

A spacecraft mission, named the Solar Polar ORbit Telescope (SPORT), is now under comprehensive scientific and engineering background studies in China. The SPORT mission focuses on CMEs, polar coronal holes, the fast solar wind, and energetic particles. As depicted in Figure 1, out-of-ecliptic imaging from SPORT can map the ecliptic in fine detail, and track the morphological and kinematical properties of Earth-directed CMEs. Scientific breakthroughs in the fields of CMEs, the fast solar wind, and high-latitude magnetism are expected, when both remote-imaging and in-situ observations from a solar polar orbit become available. The SPORT mission was first proposed in 2004 by the National Space Science Center (NSSC) of the Chinese Academy of Sciences (CAS), and later jointly studied by the University of Science and Technology of China, the National Astronomical Observatories of CAS, as well as the China Aerospace Science and Technology Corporation[30]. SPORT was successfully incorporated into the first round of background research of the Chinese Space Science Strategic Pioneer Project in 2011[31]. The Strategic Pioneer Project fosters the next generation of Chinese space science missions, aiming to deepen our understanding of the universe and Earth through independent and cooperative science programs. The roadmap of the SPORT mission includes: (i) key technology and engineering feasibility studies from 2008 to 2011, with the support of China National Space Administration, (ii) background scientific and engineering studies from 2011 to 2015, with the support of CAS, (iii) engineering implementation expected to start in 2016, if selected, (iv) tentative launch in March 2020. The science definition, orbit design, payload fabrication, and international cooperation constitute the key elements of the current SPORT blueprint.

This paper presents an overview of the SPORT mission and the accomplishment of the ongoing SPORT project, and demonstrates the scientific importance of the mission for space weather and solar physics. The scientific objectives, scientific payloads, spacecraft orbit, spacecraft platform, and international cooperation of the SPORT mission are respectively elaborated in Sections 1∼5. The status and vision of the SPORT mission within the International Living With a Star (ILWS) framework are summarized and discussed in Section 6.

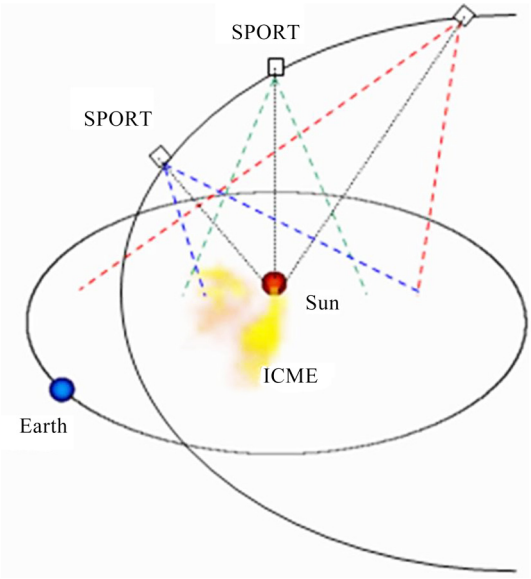

Fig. 1 An out-of-ecliptic view of the Sun and interplanetary space from the SPORT spacecraft. The three-dimensional density visualization of an interplanetary CME is generated by a time-dependent tomographic reconstruction algorithm at University of California, San Diego[32]

1 Scientific Objectives

The definition of science objectives and the prescription of payload configuration are a priority to develop the SPORT mission. The determination of science goals justifies the exploration significance and scientific merits of the SPORT mission, and also provides guidance for optimizing technical parameters of the payload design. The SPORT mission is specifically designed to target the unsolved mysteries of solar and heliospheric physics and potential application to space weather. The SPORT mission addresses the following four top-level scientific questions.

(1) Characterize CME propagation through, and interaction with, the inner heliosphere, in particular a global view of the longitudinal dimension that is so far integrated by all observations:

- Tracking kinematical motions of Earth-directed CMEs and probing these underlying dynamics;
- Coordinated studies between remote-sensing imaging and in-situ measurements of Earth-directed CMEs;
- Panoramic imaging of background solar wind streams near the ecliptic such as Corotating Interacting Regions (CIRs) and the slow solar wind.

What are the physical processes involved in the triggering, formation, propagation, and evolution of CMEs in the inner heliosphere? How do CMEs interact with the medium in the inner heliosphere, and affect its global structures and dynamics? How do the mass and magnetic field distribute in the longitudinal dimension, and whether/how are CMEs deflected in the longitudinal direction?

(2) Discover solar high-latitude magnetism associated with eruptions and solar cycle variation:

- Causal link between the solar polar magnetic field and the solar cycle variation;
- Evolution of solar high-latitude magnetic configuration before and after CME occurrence;
- Dynamic responses of the global solar atmosphere to the local CME initialization in the low corona.

How does the high-latitude magnetic field constrain the global coronal magnetic field configuration? How does the high-latitude magnetism give rise to eruptions (in particular the relationship between pseudo-streamers and sympathetic eruptions)? How does the polar magnetic field regulate solar cycle variation?

(3) Investigate the origin and properties of the fast solar wind:

- Source regions of the fast solar wind in the polar coronal holes and magneto-fluid properties of the nascent solar wind;
- Kinetic-scale waves and turbulence in the fast solar wind;
- Solar wind flows and transients around coronal streamers.

What is the structure and magnetism of the source regions that produce the fast solar wind? How do the kinetic properties of the fast solar wind connect with in-situ fluctuations/turbulence? How do the kinetic properties of the fast solar wind connect with the solar source regions?

(4) Understand the acceleration, transport, and distribution of energetic particles in the corona and heliosphere:

- Spectrum, species, and flux of energetic particles in the high-latitude heliosphere;
- Heliocentric height and spatial location of CME-driven shock formation, energetic particle acceleration across the shock front, and ensuing electromagnetic radiation from the shock front;
- Physical link between solar eruption and energetic particles.

What are the physical mechanisms of the acceleration, transport, and distribution of energetic particles in the corona and heliosphere? What is the causal relation between energetic particles and solar eruptions? In particular, how does an Energetic Neutral

Atom (ENA) imager improve our knowledge about acceleration and transport of energetic particles?

The CMEs are the largest transient and explosive events in the solar system. Our understanding of CME evolution and propagation has been significantly improved since the launch of the STEREO spacecraft in 2006[22]. The trajectories of CMEs in the corona and interplanetary space can be charted in three dimensions, using simultaneous and stereoscopic imaging by STEREO telescopes[33−36]. Remote-sensing and in-situ observations can be combined to obtain a global picture of CMEs and their consequences in the heliosphere. STEREO data have supported detailed comparison both of in-situ measurements with remote-sensing observations[19,37−38] and of heliospheric Magnetohydrodynamic (MHD) simulations with realistic observations[39−41]. However, some basic questions concerning CMEs remain outstanding: (i) What are the physical processes involved in the triggering, formation, propagation, and evolution of CMEs in the inner heliosphere? (ii) How do CMEs interact with interplanetary medium, and affect the structures and dynamics of the heliosphere? (iii) How do the mass and magnetic field distribute in the longitudinal dimension, and whether/how are CMEs deflected in the longitudinal direction?

The solar high-latitude magnetism plays a pivotal role in regulating the 11-year solar cycle[42−46]. The magnetic flux from high latitudes extends high enough in the solar atmosphere to be dragged out into the heliosphere by the solar wind. In contrast, magnetic flux from the low latitudes closes in the lower layers of the solar atmosphere. Further, controlled by interchange reconnection, these open field lines can reconnect and change their connection across the solar surface from time to time. The transport of magnetic flux at high latitudes and the properties of the polar magnetic field are paramount to answer the cyclic nature of solar magnetic activity[47−48]. Both the emerging magnetic flux and the ubiquitous convective flow underneath the photosphere shake and tangle magnetic field lines threading the corona. The poleward migration of solar magnetic flux is at the root of the magnetic polarity change every 11 years. The gradual evolution of magnetic footpoints on the photosphere, *i.e.*, magnetic shearing and/or rotation, can eventually result in an extremely structured and highly dynamic region above the sunspots. A super active solar region is likely to produce several CMEs within one day. It is still unclear what determines the amount of open magnetic flux from the Sun, and how open magnetic field lines are distributed at the solar surface. In particular, the mystery of polar corona holes is quite outstanding because all remote observations are made from the ecliptic so far[45,49].

The solar wind originates from the chromospheric networks[50−52], starts flowing out of the corona in magnetic funnels[53], and fills the entire heliosphere[54]. The fast solar wind (about $700\,\mathrm{km\cdot s^{-1}}$ and comparatively steady) outflows from large-scale regions of a single magnetic polarity in polar coronal holes[27−28,55]. The slow solar wind ($300\sim 500\,\mathrm{km\cdot s^{-1}}$), which emanates from magnetically complex regions at low latitudes and the periphery of coronal holes, permeates the ecliptic[56]. The balance between the fast and slow solar winds is modulated by the 11-year solar cycle. At solar maximum, this stable bimodal configuration gives way to a more complex mixture of slow and fast streams at all heliospheric latitudes, depending on the distribution of open and closed magnetic regions and the highly tilted magnetic polarity inversion line. The Heliospheric Current Sheet (HCS) is warped and deformed by a malalignment effect between the Sun's rotation axis and the Sun's magnetic axis, and the effect is even more prominent at solar maximum[57−59]. Fast and slow winds carry embedded turbulent fluctuations, and these fluctuations also display different properties depending on different solar origins. A statistical analysis of the fluctuating fields also reveals pervasive fine-scale structures (*e.g.*, discontinuities and pressure balanced structures)[60−61]. Such fluctuations are considered to be responsible for the difference in heating and acceleration between different solar wind

streams. Local kinetic processes dissipate the turbulent fluctuations and heat the plasma[61−65]. The SPORT mission is expected to discover (i) which magnetic and plasma structures in the low solar atmosphere does the fast solar wind come from, and (ii) how do the kinetic properties of the fast wind connect with the solar source regions?

Energetic particle radiation produced by solar eruption also fills the heliosphere. Energetic articles accelerated in the corona and inner heliosphere are scattered by inhomogeneities in the interplanetary magnetic field during their transport in the heliosphere[66−68]. Such a scattering process affects the particle flux at 1 AU. The turbulence scattering in the solar wind has spatial scales from millions of kilometers to below the electron gyro-radius. CME-driven shocks can produce relativistic particles on time scales of minutes[69−70], and many CMEs can convert around 10% of their kinetic energy into energetic particles. However, the longitudinal structure of CME is well constrained from ecliptic observations, and its extent has a large impact on the acceleration of energetic particles[71−72]. As a polar orbit mission, SPORT is very suitable to address the following puzzles of energetic particles: (i) How are energetic particles accelerated, transported, and distributed in the inner heliosphere? (ii) What is the causal relation between energetic particles and solar eruptions? (iii) How does an ENA imager improve our knowledge about acceleration and transport of energetic particles?

Overall, the SPORT mission focuses on CMEs, high-latitude magnetism, the fast solar wind, and energetic particles. Most of previous observations are made within the ecliptic. The out-of-ecliptic Ulysses spacecraft did not have remote imaging instruments[26]. Scientific breakthroughs in the fields of solar physics, heliospheric physics, and space weather are expected, when both remote-imaging and in-situ observations from a solar polar orbit become available.

2 Scientific Payloads

The SPORT scientific objectives determine the choice of scientific payloads. Space physics research is largely driven by space-based measurements, the correct interpretation of these measurements requires not only an understanding of the physics of what is being measured, but also an understanding of the experimental techniques used to obtain the measurements. The SPORT makes in-situ measurements of the solar wind plasma, electromagnetic fields, electromagnetic waves, and energetic particles from a solar polar orbit. Moreover, these in-situ measurements are connected back to their source regions on the Sun, through simultaneous remote imaging observations out of the ecliptic.

Carrying both in-situ and remote-sensing instruments at high heliospheric latitudes, SPORT addresses a central question of heliophysics: How does the Sun create and control the heliosphere? Table 1 maps the science questions to the required observations. Table 2 summarizes the mass, power, and date rate of the payloads. Final selection of the payloads is decided by the following factors: (i) capability of current and near-future Chinese instrument technology; (ii) resources of weight, power, and data rate allocated by spacecraft platform engineering; (iii) international assistance on the full or part of instrument hardware; (iv) interface between the instruments and the platform (command/control, power supply, *etc*).

Information-gathering in space is an expensive, demanding scientific endeavor that requires unique instrument design and fabrication. A suite of SPORT payloads is expected to detect the radiation, particles, waves, and fields in the inner heliosphere. The solar EUV imager aboard SPORT is designed to operate at two wavelengths of 121.6 nm and 13.1 nm. Ultraviolet coronagraph observations of the extended solar corona provide detailed empirical descriptions of coronal holes, streamers, and CMEs. In particular, the core of CMEs made of cool prominence material can be

imaged in the Lyman-α line of hydrogen atom at 121.6 nm. The simultaneous coronagraph imaging at two-channel wavelengths of visible light and 121.6 nm is realized *via* a combination of broad-band coating on the mirrors and spectral band-pass filters. The solar atmosphere from the photosphere to the corona can be continuously monitored for detecting large-scale solar eruptive events, using a set of EUV imager and coronagraph[23]. A white-light Heliospheric Imager (HI) can image both the quasi-steady flow and transient disturbances in the solar wind over a large portion of the inner heliosphere[24,73−76]. The longitudinal structures of solar storms are not observable from the ecliptic. Remote-sensing imagers aboard SPORT will provide the first-ever images of the solar polar regions and the ecliptic from an out-of-ecliptic viewpoint. Using these imaging suite, SPORT can address outstanding scientific questions, including (i) the radial dependence of CME-driven shocks and associated particle populations, (ii) the evolution of CMEs and CIRs in the inner heliosphere, (iii) the structure and turbulence within solar wind streams and their implication for the origin and evolution of the solar wind, (iv) sources, acceleration mechanisms, and transport processes of solar energetic particles. In addition, the particle detectors for the solar wind species can provide comprehensive in-situ measurements of the solar wind plasma including high time-resolution velocity distributions and composition of solar wind ions and electrons up to suprathermal energies[77−78]. Using suprathermal particles to trace interplanetary magnetic field lines, the interplanetary magnetic connectivity can be inferred. Using both particle and wave detectors, the solar wind can be comprehensively diagnosed for its properties such as the speed, mass flux, composition, magnetic field, charge states, and waves/turbulence. A three-dimensional solar-interplanetary MHD model based on a Conservation Element/Solution Element scheme[79−82] has been extensively used in synthesi-

Table 1 Description of the potential instruments aboard SPORT according to the SPORT scientific objectives

scientific objectives	required measurements
characterize CME propagation through, and interaction with, the inner heliosphere, in particular a global view of the longitudinal dimension that is so far integrated by all observations	full-disk photospheric magnetic field full-disk EUV imaging white-light imaging for the corona and heliosphere radio burst detecting in-situ measurements of plasma and magnetic field interplanetary radio imaging (optional)
discover solar high-latitude magnetism associated with eruptions and solar cycle variation	full-disk photospheric magnetic field full-disk EUV imaging white-light imaging of the corona
investigate the origin and properties of the fast solar wind	full-disk photospheric magnetic field full-disk EUV imaging white-light imaging of the corona and heliosphere in-situ measurements of plasma, magnetic field, and electric field in-situ measurements of solar wind turbulence
understand the acceleration, transport, and distribution of energetic particles	radio burst detecting white-light imaging for the corona and heliosphere in-situ measurements of energetic ions, electrons, and neutral atoms in-situ measurements of solar wind turbulence

Table 2 Mass, power, and data rate of the potential instruments

observation	instrument	mass/kg	power/W	data rate/(kbit·s^{-1})
coronal and heliospheric imaging	large-angle coronagraph (white-light and 121.6 nm)	20	25	31
	heliospheric imager	20	25	10
	energetic neutral atom imager	10	10	3
solar imaging	solar vector magnetograph	60	40	25
	solar EUV imager (121.6 nm+13.1 nm)	15 + 15	40	168
particle detecting	energetic particle and composition analyzer	11	20	5
	solar wind plasma analyzer	10	16	4
	solar wind electron detector (0.001∼3 keV + 2∼100 keV)	1 + 1	1 + 1	0.5 + 0.5
wave detecting	fluxgate magnetometer	2.5	6	1
	low frequency electromagnetic wave detector	5	5	4.6
	radio burst detector	15	18	2
	synthetic aperture radio imager (optional)	104	120	3

zing and investigating the observable signatures during the SPORT mission lifetime.

The SPORT mission has formed teams for different payloads, working on the design, fabrication, and test of the payloads. Each SPORT payload working team consists of both scientists and engineers, seeking a combination of expertise in science and engineering. Below is a list of some completed instrument prototypes.

2.1 Key Technology of Synthetic Aperture Radio Imager (SARI)

Radio signatures from interplanetary CMEs as results of thermal free-free emission and non-thermal gyro-synchrotron emission are thought to be observable[83−84]. A SARI with passive interference is designed to capture radio pictures of CMEs and trace their interplanetary propagation, using 8 long booms to perform a clock-scanning sampling of radio emission[85−87]. A 4+4 arm configuration of the 8 booms is helpful to increase the radiometric resolution and keep the system balance. Figure 2 gives the complete system design of the SARI, including antenna, receiver, and central unit. The SARI has a central frequency of 150 MHz, a bandwidth of $\geqslant$ 20 MHz, a polarization of both circular and H-V linear patterns, a Field of View (FOV) of $\pm 25^\circ$, an angular resolution of 2°, a radiometric sensitivity of $\leqslant$ 1 K, and an image refreshing time of $\leqslant$ 30 min. Image retrieval and post-processing algorithms are developed, and parts of electronic components of the SARI hardware is tested.

2.2 Prototype of White-light HI

Heliospheric imaging fills the observation gap between near-Sun coronagraph imaging and in-situ

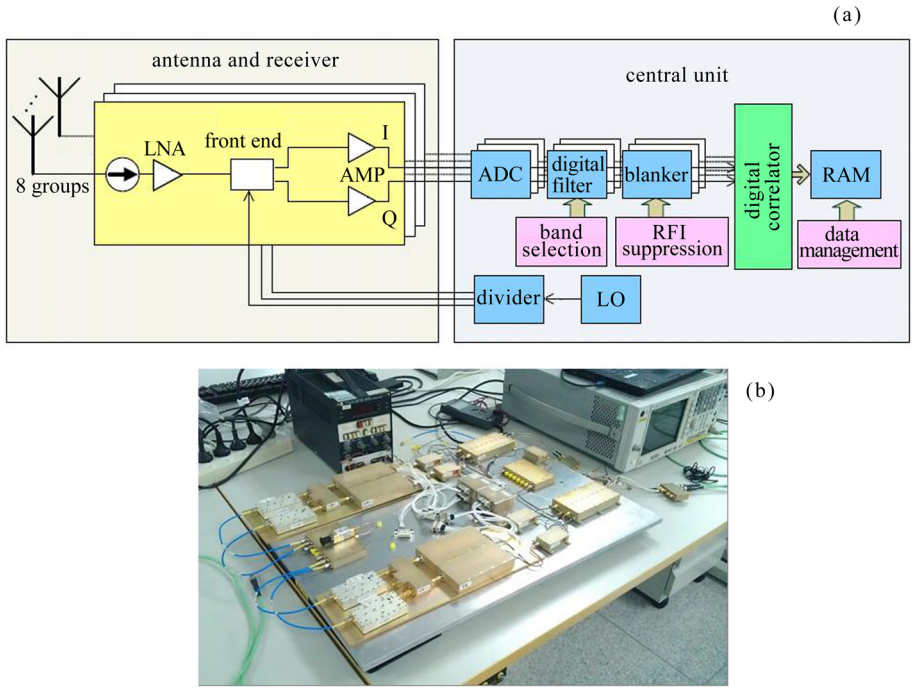

Fig. 2 System design (a) and ground experiment (b) of a synthetic aperture radio imager

measurements[24]. The angle between the Sun and a target, such as a CME, as viewed from an observer, is termed elongation ε. Interplanetary structures and transients have been viewed by means of Thomson-scattered sunlight[40,75,88]. The brightness difference between the Sun and a target (to be observed) at a large elongation is many orders of magnitude. Specifically, large CMEs at $\varepsilon = 45°$ have optical intensities that are of $10^{-14}B_{\rm s}$ order[89], where $B_{\rm s}$ is the mean solar brightness. To image interplanetary CMEs, the faint and transient signals of CMEs must be separated from many other intense and stable sources: background light from the Sun, zodiacal light, and star light. Instrument specifications for a HI aboard a deep-space spacecraft require careful design that takes into account the stray-light impacts of the imager bus, imager appendages, and other instruments[24,90−91]. A prototype of the SPORT/HI is nearly finished, as shown in Figure 3. The SPORT/HI is composed of four stops, two occulters, three groups of lenses, and a Lyot spot. A toothed occulter and diaphragm can be used to suppress stray light because they diffract much less light in the central area than a circular disk[92]. The SPORT/HI is essentially a wide-field coronagraph, following the overall optical design of the SOHO/LASCO/C2 coronagraph[93]. The SPORT/HI has a brightness sensitivity of $10^{-14}B_{\rm s}$, a FOV of ±20°, a CCD array of 2048×2048 pixels, a bandwidth of 630∼730 nm, and an angular resolution of 1.2 arcmin per pixel. The optical axis of the SPORT/HI points towards the Sun, whereas that of the STEREO/HI is off the Sun-spacecraft line. The Sun is externally occulted in the center of the SPORT/HI FOV. Accordingly, the SPORT/HI FOV covers 8∼72 $R_{\rm s}$ (24∼215 $R_{\rm s}$), when the SPORT is at 1 AU (3 AU). In contrast to the STEREO/HI, the technical difficulty of cutting the stray-light is much greater for the SPORT/HI.

2.3 Prototype of Solar EUV Imager

An EUV imager with its normal-incidence multilayer-coated optics can probe spectral emission lines at different temperatures, and diagnose the lower solar atmosphere on a global scale[94]. An EUV imager

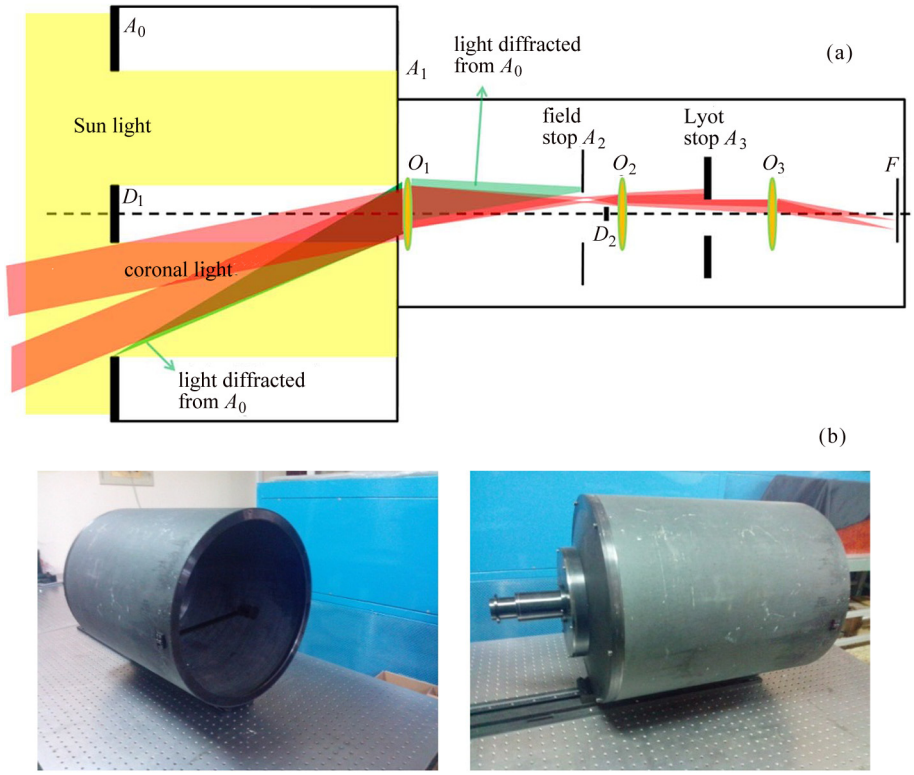

Fig. 3 Optical system design (a) and prototype (b) of a heliospheric imager. The imager consists of external diaphragm A_0, external occulter D_1, entrance aperture A_1, objective lens O_1, field stop A_2, internal occulter D_2, field lens O_2, Lyot stop A_3, relay lens with Lyot spot O_3 and focal plane F[92−93]

aboard SPORT is proposed to operate at two wavelengths, *i.e.*, 121.6 nm and 13.1 nm. The emission at 121.6 nm comes from the top of the chromosphere and the bottom of the transition layer, whereas that at 13.1 nm originates from the high corona. The SPORT/EUV imager is composed of mirrors, filters, and a focal system[95−96]. The EUV imager has a FOV of 45 arcmin, a CCD array of 2048×2048 pixels, and an angular resolution of 1.4 arcsec per pixel. The diameters of the primary and secondary mirrors are 100 mm and 38 mm, respectively. Distance between the primary and secondary mirrors is 520 mm. The structure model and optical mirrors are shown in Figure 4.

2.4 Key Components of Solar Vector Magnetograph

A full-disk photospheric magnetograph can be used to study the solar magnetic field and surface motions, and identify precursors of solar disturbances for space-weather forecasts[97−98]. The solar vector magnetograph aboard SPORT is designed on basis of multiple Lyot-type birefringent filters[99], as shown in Figure 5. The SPORT magnetograph instrument consists of three subsystems of optical imaging, optical polarimeter, and CCD readout. The diameter, focal length, and FOV of the magnetograph are 80 mm, 1000 mm, and 33 arcmin, respectively. The working wavelength of the optical subsystem is centered around 532.4 nm with a Full Width at Half Maximum (FWHM) of 0.1 Å. The incidence light inside the birefringent filter is less than 1.2°. Other technical parameters of the optical subsystem include the total transmission ($> 8\%$), off-band stray light ($< 15\%$), and working temperature ($25\pm0.01°$). The four Stokes parameters (I, Q, U, V) of the polarized sunlight from the photosphere are retrieved *via* a rapid polarization modulation[99−100]. The polarization modulation is realized through a coordinated

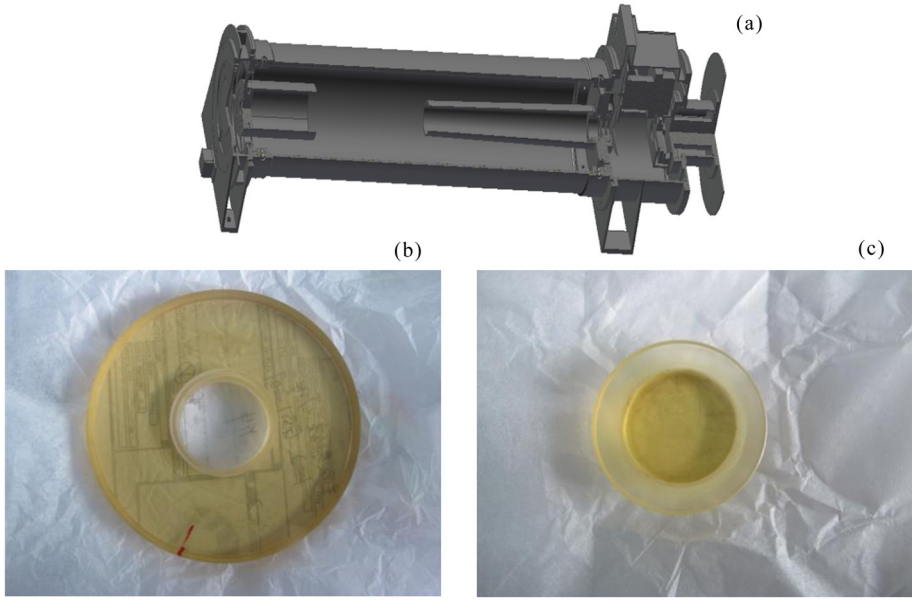

Fig. 4 Structure model (a) and primary (b)/secondary (c) mirrors of an EUV imager

combination of quarter-wavelength retardation waveplates, KD*P electro-crystals, and polarizers. Particularly, the optical subsystem should be carefully assembled and sealed to avoid any tiny air bubbles and possible silicon oil leakage.

3 Spacecraft Orbit

The orbit design is crucial to achieve the scientific objectives of SPORT. The most critical parameter of the SPORT orbit is the out-of-ecliptic inclination angle. Other factors, such as the launch vehicle, launch time window, and gravity assist, should also be considered for the orbit design. The capability of the launcher and the weight of the payloads significantly restrict the inclination angle. In order to realize the scientific objectives, the following requirements have to be satisfied: (i) the inclination angle of a desired polar orbit should be no smaller than 60°; (ii) the periapsis of the polar orbit to the Sun should be within 0.5∼1 AU; (iii) the orbit should be small enough to have a maximal time of imaging observations; (iv) the launch time should be within a solar maximum, when solar activities such as CMEs are much more frequent.

The design and optimization of the SPORT orbit are based on the successful lessons learned from the previous Ulysses[26] and the planned Solar Orbiter[101] missions. SPORT is designed to have a solar polar orbit with a gravity assist from Jupiter, similar to Ulysses[102]. In addition, the gravity of planets in the inner heliosphere can also be considered for spacecraft orbit design. Using multiple Venus flybys, the planned Solar Orbiter mission is believed to reach an inclination angle of 36°[101]. Without remote imaging instruments, Ulysses has a mass of 370 kg, a power of 285 W, and an orbit inclination of 80°[26]. In contrast to Ulysses, SPORT is much heavier in the spacecraft mass and lower in the inclination angle. For remote sensing studies of CMEs at lower heliospheric latitudes, the SPORT's inclination angle of 60°∼70° is satisfactory.

A Chinese CZ-5E rocket with upper stage is envisioned to be the launch vehicle for SPORT. As for the rocket restriction, hyperbolic excess velocity relative to the Earth should be no more than 10.5 $\mathrm{km\cdot s^{-1}}$ (Jupiter C_3 parameter is no more than 109 $\mathrm{km^2\cdot s^{-2}}$). Because of the rocket capability, the total mass of

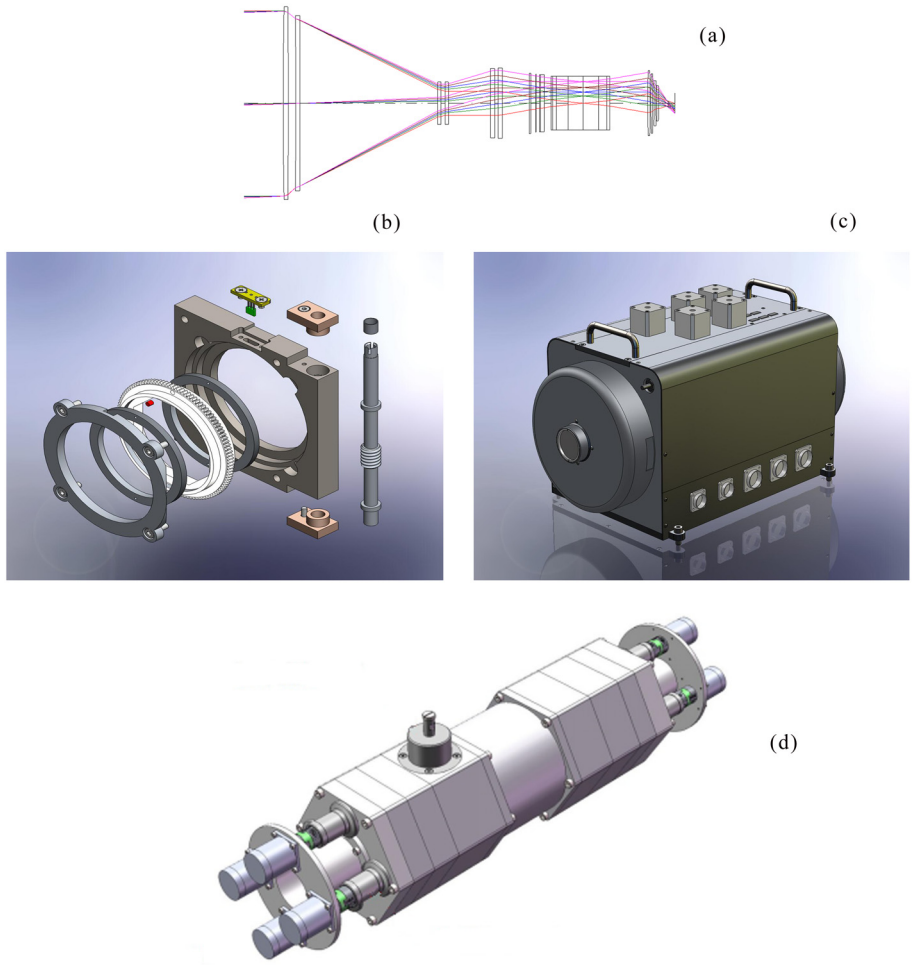

Fig. 5 Optical system design (a) and mechanic prototype (b)∼(d) of a vector magnetograph on basis of birefringent filters

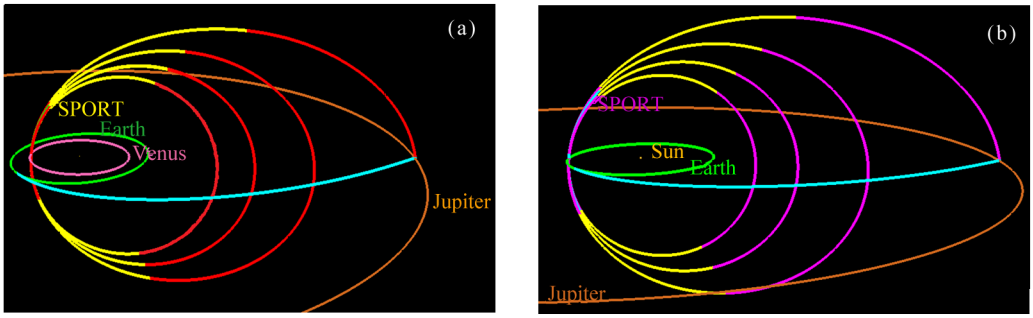

Fig. 6 SPORT orbit can be shrunk *via* Jupiter-Venus flyby (a) or Jupiter-Earth flyby (b). The yellow sections of SPORT orbits denote the working time of remote-imaging instruments

SPORT is about 1050 kg for $C_3 = 109\,\mathrm{km^2{\cdot}s^{-2}}$ and 1250 kg for $C_3 = 102\,\mathrm{km^2{\cdot}s^{-2}}$. About 150 kg of fuel is included in the spacecraft for orbit control and modification. The launch window for SPORT is intended to be March, 2020. The SPORT is designed to first travel along a big elliptic transfer orbit towards Jupiter. Using the gravity assist of Jupiter, the SPORT mission can achieve an elliptic polar orbit around

the Sun with an inclination angle of 62°, a perihelion at 0.7 AU, an aphelion at 5 AU, and an orbit period of 5 years. Imaging observations of the Sun and interplanetary space will be activated, when SPORT is within 2 AU from the Sun. For one full orbit period of 5 years, the imaging observation time is nearly 9 months (*i.e.*, from July 25, 2023 to April 13, 2024). In order to prolong the imaging observation time, further multiple gravity assists from Venus or Earth are explored to shrink the solar polar orbit within 2 AU and increase the inclination angle towards 70°. As shown in Figure 6, Table 3, and Table 4, using additional Venus (or Earth) swing-by, the imaging observation time can be extended by 25 (or 31) months during the SPORT lifetime of 10 years.

4 Spacecraft Platform

Resources needed to build and operate the spacecraft, such as mass, power, memory, and telemetry rate are always at a premium. The very worthy desire for more science per dollar has increased the demand on instrument performance while reducing resources available to the designer. Independent designs of the spacecraft are being carried out by the Beijing Institute of Spacecraft System Engineering and the Shanghai Institute of Satellite Engineering which have delivered more than 90 spacecrafts since 1970. The general parameters of the proposed SPORT spacecraft platform are given in Table 5. Specially, SPORT must be a three-axis stabilized spacecraft with a sufficient

Table 3 Gravity assists from Jupiter-Venus flyby at $C_3 = 102\,\mathrm{km^2 \cdot s^{-2}}$

flyby	time and attitude	aphelion/AU	orbit period	inclination/(°)	$\Delta v/(\mathrm{m \cdot s^{-1}})$
Jupiter flyby	epoch: 2021-08 altitude: 630 000 km	5	4.9 years (1787 days)	62.5	0
Venus flyby sequence	1st flyby epoch: 2023-12 altitude: 1860 km	3.5	3.1 years (1122 days)	64	0
	2nd flyby epoch: 2027-01 altitude: 1850 km	2.6	2.1 years (780 days)	65.5	44
	3rd flyby epoch: 2031-04 altitude: 2000 km	2.0	1.6 years (600 days)	67	67

Table 4 Gravity assists from Jupiter-Earth flyby at $C_3 = 102\,\mathrm{km^2 \cdot s^{-2}}$

flyby	time and attitude	aphelion/AU	orbit period	inclination/(°)	$\Delta v/(\mathrm{m \cdot s^{-1}})$
Jupiter flyby	Epoch: 2021-08 altitude: 626 000 km	5	5.2 years (1912 days)	61.5	0
Earth flyby sequence	1st flyby epoch: 2024-02 altitude: 2550 km	3.2	3.0 years (1094 days)	64.3	0
	2nd flyby epoch: 2027-02 altitude: 2378 km	2.2	2.0 years (730 days)	66.7	73
	3rd flyby epoch: 2029-02 altitude: 2380 km	1.6	1.5 years (538 days)	69.3	2

pointing accuracy; SPORT must satisfy electromagnetic cleanliness such that the imaging, particle, and wave detectors can accurately measure relevant physical parameters; SPORT must combine China's existing tracking infrastructure and worldwide facilities to achieve the requirements of tracking, operations, and data downlink. The SPORT payload configuration is designed with two platform models and illustrated in Figure 7. Because of high orbit inclination, the total mass of SPORT has to be no more than 1050 kg. If a lower orbit inclination is acceptable, SPORT can accommodate more propellant for orbit maneuver and/or more mass for payloads.

The design of the spacecraft platform includes many aspects such as the structure, mechanisms, thermal control, material, propulsion, electronic components, and so on. The SPORT measurements to achieve the scientific objectives place the following requirements on the spacecraft engineering.

4.1 Multi-source Hybrid Power Supply and Advanced Active Thermal Control

SPORT, travelling at an elliptic orbit around the Sun,

Table 5 Parameters of SPORT spacecraft platform

item	parameter	range
system parameters	lifetime/a	10
	mass/kg	1050
payload	mass/kg	$\leqslant 120$
	power/W	$\leqslant 132$
structure and mechanism	size/mm	1780×1980×2650
	first-order frequency in launching state/Hz	transverse > 15, longitudinal > 30
	structure bearing capacity/kg	1200
GNC	control model	3-axis stabilized
	pointing accuracy (to the Sun)	$20''$ (3σ)
	attitude stability	$1.5''/10$ s (3σ)
propulsion	propellant/kg	hydrazine about 200
	I_{sp}/s	220
power	voltage/V	29±1
	RTG/W	40
	RTG efficiency	10%
telecommunication	TM bit rate/(bit·s^{-1})	16∼65 536
	TC bit rate/(bit·s^{-1})	7.8125, 125, 2000
	storage/Tbit	8
	carrier frequency	X Band
	TT&C modulation	PCM-PSK-PM
	ranging type	ranging tone + pn/PN sequence
	transmitter power/W	100 (X band), 100 (Ka band)
	transmission model	BPSK
	transmission bit rate/(kbit·s^{-1})	20∼500

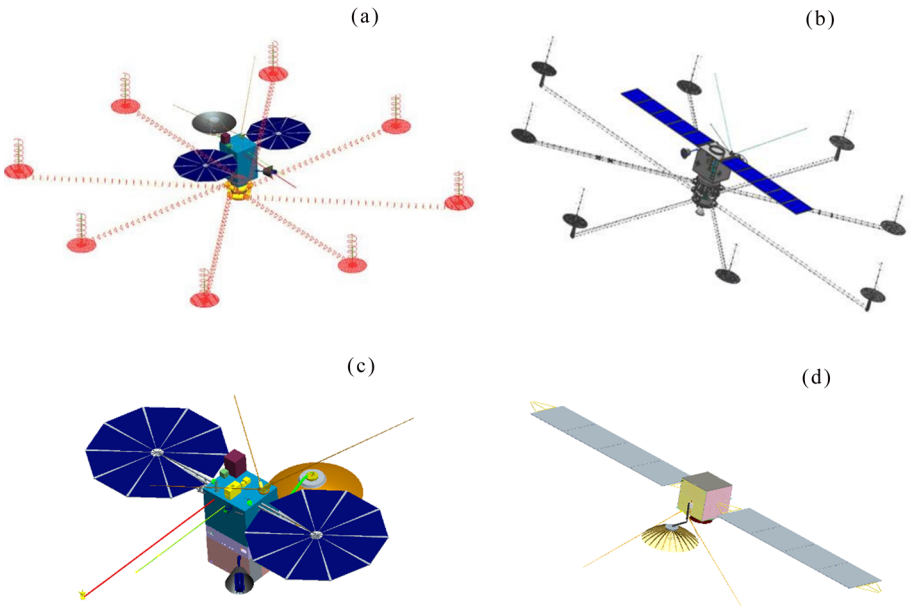

Fig. 7 SPORT platform models independently designed by the Beijing Institute of Spacecraft System Engineering (a) (c) and the Shanghai Institute of Satellite Engineering (b) (d). Because of the high risks and technology difficulties, a synthetic aperture radio imager is likely to be excluded from the SPORT payload list. Accordingly, the SPORT platform designs are simplified from the models (a) (b) to (c) (d)

will undergo a dramatic change of the solar luminous flux from 51 to 2800 $\mathrm{W{\cdot}m^{-2}}$. The ambient environment around SPORT is cold near Jupiter and hot near Sun. As the solar panel cannot supply necessary power near Jupiter, an RTG is now considered for an additional power source. The RTG technique has been successfully applied to the Chinese Chang'E-3 lunar mission in late 2013[103]. But the mixed use of solar panel and RTG is unprecedented and challenging for the Chinese industry.

4.2 Design of Large Booms Deployable in Space

The long booms aboard SPORT has low mass, low stiffness, weak damping, and dense vibration modes. There is a strong coupling between boom vibration and attitude control. The stability of the flexible deployable booms and its coupling dynamics with the spacecraft platform are being analyzed. Thermal deformation of the booms should be minimized to maintain high accuracies of the pointing and stability. Composite material such as carbon fiber is considered to be used to make these booms.

4.3 Attitude Stability and Control For a Flexible Probe

The antenna booms and large solar panels make SPORT as a flexible probe. Moreover, high pointing accuracy of $20''$ (3σ) is demanded by the performance of scientific instruments. Now, the attitude dynamics of the flexible probe, coupling with vibration modes of solar panels and deployed booms, is intensively studied. A suitable controller is being designed to control the attitude of platform and suppress the vibration of deployed booms and solar panels.

4.4 Deep Space Communication

The distance between the spacecraft antenna and terrestrial receiver could be as far as 9×10^8 km. Even for a minimal configuration of the scientific instruments, the data rate reaches 45 $\mathrm{kbit{\cdot}s^{-1}}$. In order to transmit the data from SPORT, key microwave devices, such as dielectric resonator oscillator with low phase noise, low power amplifier, *etc.*, are being fabricated, and advanced technology of weak signal acquisition

and adaptive phase-locked receiver are being developed.

5 International Cooperation

Space science is an extremely costly enterprise and the budgets will always be limited, so the heliospheric missions should be coordinated to maximize the science return. Only by working together and coordinating efforts, the international space science community can make the most out of the limited resources. SPORT, together with Solar Probe Plus, Solar Orbiter, and InterHelio-Probe, are now incorporated together under an ILWS framework for the purpose of coordinated exploitation of the inner heliosphere[104]. The orbits of the Solar Probe Plus[105−106], Solar Orbiter[101,107], InterHelio-Probe[108−109], and Solar Polar Imager[110−111]are depicted in Figure 8, and their science goals are summarized in Table 6.

Coordinated observations between the SPORT and other spaceborne/ground-based facilities would greatly enhance scientific outputs. Each of these missions had a specific focus, being part of an overall strategy of coordinated solar and heliospheric research[104]. For example, a white-light HI aboard SPORT at high heliospheric latitudes has a FOV that can encompass the spacecraft orbits of Solar Probe Plus and Solar Orbiter, which is crucial to provide a contextual link for in-situ and remote-sensing instruments aboard other spacecraft at low heliospheric latitudes. In the STEREO era, a CME can be imaged from its nascent stage in the inner corona all the way out to 1 AU and beyond, but this is viewed from the ecliptic. With SPORT, CMEs can be imaged from an out-of-ecliptic viewpoint. Particularly, the out-of-ecliptic imaging from the SPORT has a FOV, covering the orbits of Solar Orbiter, Solar Probe Plus, and InterHelio-Probe. The synergy between SPORT, Solar Probe Plus, Solar Orbiter, and InterHelio-Probe can simultaneously explore the inner heliosphere in three dimensions and make major breakthroughs in the connections and coupling between the Sun and the heliosphere.

6 Summary and Conclusions

SPORT will carry a suite of remote-sensing and in-situ instruments to observe the CMEs, solar high-

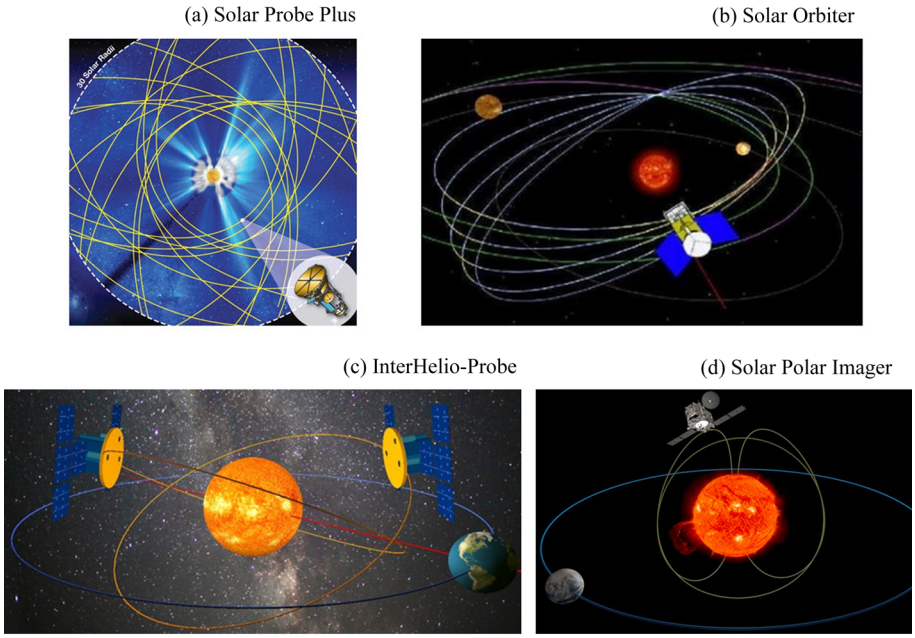

Fig. 8 Planned orbits of four future spacecraft missions

Table 6 A brief introduction to some planned/proposed heliospheric exploration missions

mission	description	scientific goals
Solar Probe Plus (NASA)	approach within 8.86 solar radii to the photosphere survive the harsh environment near the Sun, using a solar shadow-shield to withstand the intense heat and radiation probe the outer corona locally	structure and dynamics of the magnetic fields at the sources of the solar wind flow of energy that heats the corona and accelerates the solar wind acceleration and transport of energetic particles dusty plasma near the Sun and its influence on the solar wind and energetic particle formation
Solar Orbiter (ESA)	make observations of the Sun from an eccentric orbit moving as close as about 60 solar radii, placing it slightly inside Mercury's perihelion and from up to 30° above the ecliptic perform detailed measurements of the inner heliosphere and nascent solar wind	origin of the solar wind plasma and magnetic field in the corona heliospheric variability driven by solar transients energetic particle radiation produced by solar eruptions solar dynamo and its connections between the Sun and the heliosphere
InterHelio-Probe (Russia)	after a short ecliptic phase, the gravity-assisted maneuvers at Venus will be used for maximal inclination of the orbit to the ecliptic with a possible second spacecraft, InterHelio-Probe will be transformed into a PEP (Polar Ecliptic Patrol) mission	mechanisms of the solar corona heating and acceleration of the solar wind fine structure and dynamics of the solar atmosphere nature and global dynamics of the solar flares and CMEs and their influence on the heliosphere and space weather energetic particles powerfully and changeably accelerated by the Sun solar atmosphere in polar and equatorial regions
Solar Polar Imager (NASA)	use a solar sail to leave the ecliptic, and reach high inclination angle of about 75° heliocentric orbit at 0.5 AU observe solar activities from a new perspective of solar polar orbit	helioseismology and magnetic fields of polar regions polar view of corona, CMEs, and total solar irradiance link high-latitude solar wind and energetic particles to coronal sources

latitude magnetism, fast solar wind, and energetic particles from a polar orbit around the Sun. SPORT is intended to be the first mission that carries remote-sensing instruments (complemented with in-situ detectors) from a polar orbit around the Sun, the first mission that could image interplanetary CMEs at radio wavelengths from space, and the first mission that could measure solar high-latitude magnetism leading to solar eruptions and fast solar wind. SPORT would provide a unique opportunity to study CME propa-

gation through the inner heliosphere from a vantage point at high latitudes and investigate solar high-latitude magnetism giving rise to solar eruptions and fast solar wind.

Tentative payloads aboard SPORT include a solar EUV imager (121.6 and 13.1 nm), a solar vector magnetograph, a large-angle coronagraph (white-light and 121.6 nm), a HI, an energetic neutral atom imager, a solar wind plasma analyzer, a fluxgate magnetometer, a radio burst detector, a low-frequency electromagnetic wave detector, and an energetic particle and composition analyzer. The tradeoff between the polar orbit inclination and the payload mass has to be considered in terms of cost-performance balance. Risks should also be carefully taken into account, in particular for a synthetic aperture radio imager. If more payload mass is allowable, additional instruments such as the synthetic aperture radio imager could be mounted on the SPORT platform.

The current background studies of the SPORT mission aim at being competitively selected and officially approved during China's 13th Five-Year Plan period of 2016—2020. If successfully approved, the SPORT mission will be boosted from the background phase to the engineering phase. Meanwhile, the development of the SPORT mission continues with the goal of a launching around 2020. The scientists and engineers should be coordinated to ensure scientific merits and technique feasibilities for each payload. All risks in instruments, platform, and rocket should be avoided or minimized within a reliable technology readiness level.

International collaboration is vital for the development of the SPORT mission. China has an open-door policy regarding international collaboration in space science. Both of the earlier Chinese space-science missions had a strong component of international collaboration: Double Star was a joint mission between China's National Space Administration and ESA[112]; Yinghuo-1 was launched through the Russian Phobos-Grunt mission — although the spacecraft failed to leave Earth's orbit[113]. The SPORT team benefits greatly from the invaluable legacy inherited from developing the past Chinese missions of Double Star and Yinghuo-1. However, there is still a lack of trial-and-error development and space flight experience in China, especially at the payload level. International partnerships for instrumentation designs and scientific collaborations are both needed and welcome.

Heliospheric satellite missions should be coordinated within the ILWS framework. An ILWS task group on coordinating future missions of the Solar Probe Plus, Solar Orbiter, SPORT, and InterHelio-Probe was established in September 2013. The SPORT mission is complementary to other inner heliospheric missions. The concurrent science operations of the Solar Orbiter, Solar Probe Plus, SPORT, and InterHelio-Probe missions will offer a truly unique epoch in heliospheric science. While each mission will achieve its own important science objectives, coordination of these spacecraft will be capable of doing the multi-point measurements required to address many mysteries in heliophysics such as the coronal origin of the solar wind plasma and magnetic field or the way in which the solar transients drive the heliospheric variability.

Acknowledgement This paper is adapted from an internal report of the International Space Science Institute in Beijing (ISSI-BJ) Magazine of No.4 in August, 2014. The majority of this paper is an outcome of the first ISSI-BJ SPORT Forum in 2013. The forum was essential in defining the scientific goals of the SPORT mission and for maintaining the international community involvement. Ming Xiong would like to sincerely thank Prof. Roger Bonnet, Maurizio Falanga, Jean-Claude Vial, and Angelos Vourlidas for their constructive comments on the previous ISSI-BJ SPORT report.

References

[1] National Science and Technology Council. National Space Weather Program Strategic Plan [M]. Washington: Office of the Federal Coordinator for Meteorological Services and Supporting Research, 2010

[2] National Science and Technology Council. National Space

Weather Strategy: Space Weather Operations, Research, and Mitigation (SWORM) Task Force [M]. Washington: Executive Office of the President of the United States, 2015

[3] BELCHER J W, DAVIS L Jr. Large-amplitude Alfv́en waves in the interplanetary medium, 2 [J]. *J. Geophys. Res.*, 1971, **76**: 3534-3563

[4] MATTHAEUS W H, GOLDSTEIN M L. Measurement of the rugged invariants of magnetohydrodynamic turbulence in the solar wind [J]. *J. Geophys. Res.*, 1982, **87**: 6011-6028

[5] TU C Y, MARSCH E. MHD structures, waves and turbulence in the solar wind: observations and theories [J]. *Space Sci. Rev.*, 1995, **73**: 1-210

[6] LI B, LI X. Propagation of non-Wentzel-Kramers-Brillouin alfv́en waves in a multi-component solar wind with differential ion flow [J]. *Astrophys. J.*, 2007, **661**: 1222-1233

[7] FORBES T G, LINKER J A, CHEN J, *et al.* CME theory and models [J]. *Space Sci. Rev.*, 2006, **123**: 251-302

[8] GOPALSWAMY N. Properties of interplanetary coronal mass ejections [J]. *Space Sci. Rev.*, 2006, **124**: 145

[9] WEBB D F, Howard T A. Coronal mass ejections: observations [J]. *Living Rev. Solar Phys.*, 2012, **9**: 3

[10] GOSLING J T, MCCOMAS D J, PHILLIPS J L, BAME S J. Geomagnetic activity associated with Earth passage of interplanetary shock disturbances and coronal mass ejections [J]. *J. Geophys. Res.*, 1991, **96**: 7831-7839

[11] ZHANG J, RICHARDSON I G, WEBB D F, *et al.* Solar and interplanetary sources of major geomagnetic storms ($Dst \leqslant -100$ nT) during 1996—2005 [J]. *J. Geophys. Res.*, 2007, **112**(A10): A10102

[12] BURLAGA L F, BEHANNON K W, KLEIN L W. Compound streams, magnetic clouds, and major geomagnetic storms [J]. *J. Geophys. Res.*, 1987, **92**: 5725-5734

[13] BURLAGA L F, PLUNKETT S P, ST CYR O C. Successive CMEs and complex ejecta [J]. *J. Geophys. Res.*, 2002, **107**: 1266

[14] WANG Y M, YE P Z, WANG S. Multiple magnetic clouds: several examples during March—April 2001 [J]. *J. Geophys. Res.*, 2003, **108**: 1370

[15] XIONG M, ZHENG H N, WANG Y M, WANG S. Magnetohydrodynamic simulation of the interaction between interplanetary strong shock and magnetic cloud and its consequent geoeffectiveness [J]. *J. Geophys. Res.*, 2006, **111**: A08105

[16] XIONG M, ZHENG H N, WU S T, WANG Y M, WANG S. Magnetohydrodynamic simulation of the interaction between two interplanetary magnetic clouds and its consequent geoeffectiveness [J]. *J. Geophys. Res.*, 2007, **112**: A11103

[17] SHEN C, WANG Y, WANG S, *et al.* Super-elastic collision of large-scale magnetized plasmoids in the heliosphere [J]. *Nat. Phys.*, 2012, **8**: 923

[18] LIU Y, LUHMANN J G, KAJDIC P, *et al.* Observations of an extreme storm in interplanetary space caused by successive coronal mass ejections [J]. *Nat. Comm.*, 2014, **5**: 3481

[19] Liu Y, Luhmann J G, Müller-Mellin R, *et al.* A comprehensive view of the 2006 December 13 CME: from the Sun to interplanetary space [J]. *Astrophys. J.*, 2008, **689**: 563-571

[20] ZHANG M, LOW B C. The hydromagnetic nature of solar coronal mass ejections [J]. *Ann. Rev. Astron. Astrophys.*, 2005, **43**: 103-137

[21] PEVTSOV A A, BERGER, M A, NINDOS A, *et al.* Magnetic helicity, tilt, and twist [J]. *Space Sci. Rev.*, 2015, **186**: 285-324

[22] KAISER M L, KUCERA T A, DAVILA J M, *et al.* The STEREO mission: An introduction [J]. *Space Sci. Rev.*, 2008, **136**: 5-16

[23] HOWARD R A, MOSES J D, VOURLIDAS A, *et al.* Sun Earth Connection Coronal and Heliospheric Investigation (SECCHI) [J]. *Space Sci. Rev.*, 2008, **136**: 67-115

[24] EYLES C J, HARRISON R A, DAVIS C J, *et al.* The Heliospheric Imagers onboard the STEREO mission [J]. *Solar Phys.*, 2009, **254**: 387-445

[25] MARSDEN R G, WENZEL K P. The International Solar Polar Mission (ISPM) [J]. *Plasma Astrophys.*, 1981, **164**: 51-59

[26] WENZEL K P, MARSDEN R G, PAGE D E, SMITH E J. The Ulysses mission [J]. *Astron. Astrophys. Supp.*, 1992, **92**: 207

[27] SMITH E J, MARSDEN R G, PAGE D E. Ulysses above the Sun's south pole: an introduction [J]. *Science*, 1995, **268**: 1005-1007

[28] MCCOMAS D J, BARRACLOUGH B L, FUNSTEN H O, *et al.* Solar wind observations over Ulysses' first full polar orbit [J]. *J. Geophys. Res.*, 2000, **105**: 10419-10434

[29] BALOGH A, MARSDEN R G, SMITH E J. The Heliosphere near Solar Minimum: the Ulysses Perspective [R]. Chichester: Springer-Praxis, 2001

[30] WU J, SUN W Y, ZHENG J H, *et al.* Imaging interplanetary CMEs at radio frequency from solar polar orbit [J]. *Adv. Space Res.*, 2011, **48**: 943

[31] WU J, SUN L L. Strategic priority program on space science [J]. *Chin. J. Space Sci.*, 2014, **34**(5): 505-515

[32] JACKSON B V, HICK P P, BUFFINGTON A, *et al.* Three-dimensional reconstruction of heliospheric structure using iterative tomography: a review [J]. *J. Atmos. Solar-Terre. Phys.*, 2011, **73**(10): 1214-1227

[33] THERNISIEN A, VOURLIDAS A, HOWARD R A. Forward modeling of coronal mass ejections using STEREO/SECCHI data [J]. *Solar Phys.*, 2009, **256**: 111

[34] LIU Y, DAVIES J A, LUHMANN J G, *et al.* Geometric triangulation of imaging observations to track coronal

mass ejections continuously out to 1 AU [J]. *Astrophys. J.*, 2010, **710**: L82-L87

[35] LUGAZ N, HERNANDEZ-CHARPAK J N, ROUSSEV I I, *et al*. Determining the azimuthal properties of coronal mass ejections from multi-spacecraft remote-sensing observations with STEREO SECCHI [J]. *Astrophys. J.*, 2010, **715**: 493-499

[36] DAVIES J A, PERRY C H, TRINES R M G M, *et al*. Establishing a stereoscopic technique for determining the kinematic properties of solar wind transients based on a generalized self-similarly expanding circular geometry [J]. *Astrophys. J.*, 2013, **777**: 167

[37] ROUILLARD A P, DAVIES J A, FORSYTH R J, *et al*. A solar storm observed from the Sun to Venus using the STEREO, Venus Express, and MESSENGER spacecraft [J]. *J. Geophys. Res.*, 2009, **114**: A07106

[38] MOSTL C, TEMMER M, ROLLETT T, FARRUGIA C J, *et al*. STEREO and WIND observations of a fast ICME flank triggering a prolonged geomagnetic storm on 5—7 April 2010 [J]. *Geophys. Res. Lett.*, 2010, **37**: L24103

[39] LUGAZ N, VOURLIDAS A, ROUSSEV I I, MORGAN H. Solar-terrestrial simulation in the STEREO era: the 24—25 January 2007 eruptions [J]. *Solar Phys.*, 2009, **256**: 269

[40] XIONG M, DAVIES J A, BISI M M, OWENS M J, FALLOWS R A, DORRIAN G D. Effects of Thomson-Scattering geometry on white-light imaging of an interplanetary shock: synthetic observations from forward magnetohydrodynamic modelling [J]. *Solar Phys.*, 2013, **285**: 369-389

[41] XIONG M, DAVIES J A, FENG X, OWENS M J, HARRISON R A, DAVIS C J, LIU Y. Using coordinated observations in polarized white light and Faraday rotation to probe the spatial position and magnetic field of an interplanetary sheath [J]. *Astrophys. J.*, 2013, **777**: 32

[42] BABCOCK H D. The Sun's polar magnetic field [J]. *Astrophys. J.*, 1959, **130**: 364

[43] TSUNETA S, ICHIMOTO K, KATSUKAWA Y, *et al*. The magnetic landscape of the Sun's polar region [J]. *Astrophys. J.*, 2008, **688**: 1374-1381

[44] SUN X, HOEKSEMA J T, LIU Y, ZHAO J. On polar magnetic field reversal and surface flux transport during solar cycle 24 [J]. *Astrophys. J.*, 2015, **798**: 114

[45] PETRIE G J D. Solar magnetism in the polar regions [J]. *Living Rev. Solar Phys.*, 2015, **12**: 5

[46] WANG Y M, LEAN J, SHEELEY N R. Role of a variable meridional flow in the secular evolution of the Sun's polar fields and open flux [J]. *Astrophys. J. Lett.*, 2002, **577**: L53-L57

[47] CHOUDHURI A R, CHATTERJEE P, JIANG J. Predicting solar cycle 24 with a solar dynamo model [J]. *Phys. Rev. Lett.*, 2007, **98**: 131103

[48] UPTON L, HATHAWAY D H. Predicting the Sun's polar magnetic fields with a surface flux transport model [J]. *Astrophys. J.*, 2014, **780**: 5

[49] SUN X, LIU Y, HOEKSEMA J T, HAYASHI K, ZHAO X. A new method for polar field interpolation [J]. *Solar Phys.*, 2011, **270**: 9

[50] XIA L D. Equatorial Coronal Holes and Their Relation to the High-speed Solar Wind Streams [D]. Göttingen: Georg-August-University, 2003

[51] XIA L D, MARSCH E, WILHELM K. On the network structures in solar equatorial coronal holes: observations of SUMER and MDI on SOHO [J]. *Astron. Astrophys.*, 2004, **424**(3): 1025-1037

[52] TIAN H, DELUCA E E, CRANMER S R, *et al*. Prevalence of small-scale jets from the networks of the solar transition region and chromosphere [J]. *Science*, 2014, **346**: 1255711

[53] TU C Y, ZHOU C, MARSCH E, XIA L D. Solar wind origin in coronal funnels [J]. *Science*, 2005, **308**: 519

[54] PARKER E N. Dynamics of the interplanetary gas and magnetic fields [J]. *Astrophys. J.*, 1958, **128**: 664

[55] CRANMER S R. Coronal holes and the high-speed solar wind [J]. *Space Sci. Rev.*, 2002, **101**: 229

[56] FELDMAN U, LANDI E, SCHWADRON N A. On the sources of fast and slow solar wind [J]. *J. Geophys. Res.*, 2005, **110**(A7): A07109

[57] HOEKSEMA J T, WILCOX J M, SCHERRER P H. The structure of the heliospheric current sheet: 1978—1982 [J]. *J. Geophys. Res.*, 1983, **88**: 9910-9918

[58] SMITH E J. The heliospheric current sheet [J]. *J. Geophys. Res.*, 2001, **106**(A8): 15819-15832

[59] ZHAO X P, HOEKSEMA J T, SCHERRER P H. Prediction and understanding of the north-south displacement of the heliospheric current sheet [J]. *J. Geophys. Res.*, 2005, **110**(A10): A10101

[60] BURLAGA L F. Intermittent turbulence in the solar wind [J]. *J. Geophys. Res.*, 1991, **96**: 5847-5851

[61] ROBERTS O W, LI X, LI B. Kinetic plasma turbulence in the fast solar wind measured by Cluster [J]. *Astrophys. J.*, 2013, **769**: 58

[62] STIX T H. Waves in Plasmas [M]. New York: American Institute of Physics, 1992

[63] LEAMON R J, SMITH C W, NESS N F, MATTHAEUS W H, WONG H K. Observational constraints on the dynamics of the interplanetary magnetic field dissipation range [J]. *J. Geophys. Res.*, 1998, **103**: 4775

[64] BALE S D, KELLOGG P J, MOZER F S, HORBURY T S, REME H. Measurement of the electric fluctuation spectrum of magnetohydrodynamic turbulence [J]. *Phys. Rev. Lett.*, 2005, **94**(21): 215002

[65] HE J, MARSCH E, TU C, YAO S, TIAN H. Possible evidence of Alfv́en-cyclotron waves in the angle distribution of magnetic helicity of solar wind turbulence [J]. *Astrophys. J.*, 2011, **731**: 85

[66] JOKIPII J R. Cosmic-ray propagation. I. Charged parti-

cles in a random magnetic field [J]. *Astrophys. J.*, 1966, **146**: 480

[67] ZHANG M, QIN G, RASSOUL H. Propagation of solar energetic particles in three-dimensional interplanetary magnetic fields [J]. *Astrophys. J.*, 2009, **692**: 109-132

[68] MATTHAEUS W H, QIN G, BIEBER J W, ZANK G P. Nonlinear collisionless perpendicular diffusion of charged particles [J]. *Astrophys. J. Lett.*, 2003, **590**: L53-L56

[69] LEE M A. Coupled hydromagnetic wave excitation and ion acceleration at interplanetary traveling shocks [J]. *J. Geophys. Res.*, 1983, **88**: 6109-6119

[70] ZANK G P, RICE W K M, WU C C. Particle acceleration and coronal mass ejection driven shocks: a theoretical model [J]. *J. Geophys. Res.*, 2000, **105**(A11): 25079-25096

[71] REAMES D V, BARBIER L M, NG C K. The spatial distribution of particles accelerated by coronal mass ejection-driven shocks [J]. *Astrophys. J.*, 1996, **466**: 473

[72] REAMES D V, KAHLER S W, NG C K. Spatial and temporal invariance in the spectra of energetic particles in gradual solar events [J]. *Astrophys. J.*, 1997, **491**: 414-420

[73] HARRISON R A, DAVIS C J, EYLES C J, *et al.* First imaging of coronal mass ejections in the heliosphere viewed from outside the Sun-Earth line [J]. *Solar Phys.*, 2008, **247**: 171-193

[74] DAVIES J A, HARRISON R A, ROUILLARD A P, *et al.* A synoptic view of solar transient evolution in the inner heliosphere using the heliospheric imagers on STEREO [J]. *Geophys. Res. Lett.*, 2009, **36**: L02102

[75] JACKSON B, BUFFINGTON A, HICK P, *et al.* A heliospheric imager for deep space: lessons learned from Helios, SMEI, and STEREO [J]. *Solar Phys.*, 2010, **265**: 257-275

[76] DEFOREST C E, HOWARD T A. Feasibility of heliospheric imaging from near Earth [J]. *Astrophys. J.*, 2015, **804**: 126

[77] GLOECKLER G, BALSIGER H, BURGI A, *et al.* The solar wind and suprathermal ion composition investigation on the WIND spacecraft [J]. *Space Sci. Rev.*, 1995, **71**: 79-124

[78] GLOECKLER G, CAIN J, IPAVICH F M, *et al.* Investigation of the composition of solar and interstellar matter using solar wind and pickup ion measurements with SWICS and SWIMS on the ACE spacecraft [J]. *Space Sci. Rev.*, 1998, **86**: 497

[79] FENG X, YANG L, XIANG C, *et al.* Three-dimensional solar wind modeling from the Sun to Earth by a SIP-CESE MHD model with a six-component grid [J]. *Astrophys. J.*, 2010, **723**: 300

[80] FENG X, ZHANG M, ZHOU Y. A new three-dimensional solar wind model in spherical coordinates with a six-component grid [J]. *Astrophys. J.*, 2014, **214**(Supp.): 6

[81] ZHOU Y, FENG X, ZHAO X. Using a 3-D MHD simulation to interpret propagation and evolution of a coronal mass ejection observed by multiple spacecraft: the 3 April 2010 event [J]. *J. Geophys. Res.*, 2014, **119**: 9321-9333

[82] FENG X, MA X, XIANG C. Data-driven modeling of the solar wind from 1 R_s to 1 AU [J]. *J. Geophys. Res.*, 2015, **120**: 10159-10174

[83] SUN W Y, WU J. A study of the Bremsstrahlung of plasma at about 1 AU in times of quiet Sun and flare activity [J]. *Chin. Astron. Astrophys.*, 2005, **29**: 149

[84] SUN W Y, WU J. Radiation mechanisms of the plasma near point L1 affected by CMEs and associated microwave bursts [J]. *Chin. Astron. Astrophys.*, 2005, **29**: 413

[85] WU J, HUANG Y H, DONG X L. Image retrieval algorithm of two-dimensional synthetic aperture radiometer [C]//Sydney: IEEE Geoscience and Remote Sensing Symposium (IGARSS), 2001: 3268-3270

[86] LIU H, MAAGT DE P, CHRISTENSEN J, *et al.* Radiometric analysis of the rotating synthetic aperture radiometers utilizing grid-based measurement approach [C]//Barcelona: IEEE Geoscience and Remote Sensing Symposium (IGARSS), 2007: 235-238

[87] ZHANG C, WU J, LIU H, *et al.* Scan scheme and imaging algorithm of Solar Polar Orbiter Telescope (SPORT) [C]//Vancouver: IEEE Geoscience and Remote Sensing Symposium (IGARSS), 2011: 2266-2269

[88] HOWARD T A, TAPPIN S J. Interplanetary coronal mass ejections observed in the heliosphere: 1. Review of theory [J]. *Space Sci. Rev.*, 2009, **147**: 31-54

[89] DEFOREST C E, HOWARD T A, TAPPIN S J. Observations of detailed structure in the solar wind at 1 AU with STEREO/HI-2 [J]. *Astrophys. J.*, 2011, **738**: 103

[90] HARRISON R A, DAVIS C J, EYLES C J. The STEREO heliospheric imager: how to detect CMEs in the heliosphere [J]. *Adv. Space Res.*, 2005, **36**: 1512-1523

[91] ZHANG H X, LU Z W, XIA L D, LIU H, LI P. Stray light suppressing of optical system in white light coronagraph [J]. *Opt. Prec. Eng.*. 2009, **17**(10): 2371-2376

[92] SUN M Z, ZHANG H X, BU H Y, *et al.* Computation of the diffracted field of a toothed occulter by the semi-infinite rectangle method [J]. *J. Opt. Soc. Am. A*, 2013, **30**(10): 2140-2149

[93] BRUECKNER G, HOWARD R, KOOMEN M, *et al.* The Large Angle Spectroscopic Coronagraph (LASCO) [J]. *Solar Phys.*, 1995, **162**: 357-402

[94] DELABOUDINIERE J P, ARTZNER G E, BRUNAUD J, *et al.* EIT: Extreme-ultraviolet Imaging Telescope for the SOHO mission [J]. *Solar Phys.*, 1995, **162**(1/2): 291-312

[95] LI B Q, ZHU G W, WANG S J, LIN H A, *et al.* Solar X-EUV Imaging Telescope [J]. *Chin. J. Geophys.*, 2005, **48**(2): 235-242

[96] LI B Q, LI H T, ZHOU S Z, JIANG B. The Lyman-alpha imager onboard Solar Polar ORbit Telescope [J]. *Proc. SPIE*, 2013, **9042**(4): 237-244

[97] SCHERRER P H, BOGART R S, BUSH R I, *et al.* The

solar oscillations investigation — Michelson Doppler imager [J]. *Solar Phys.*, 1995, **162**: 129

[98] SCHERRER P H, SCHOU J, BUSH R I, *et al.* The Helioseismic and Magnetic Imager (HMI) investigation for the Solar Dynamics Observatory (SDO) [J]. *Solar Phys.*, 2012, **275**: 207-227

[99] WANG D G, DENG Y Y, AI G X. Analysis of a new polarimeter for space solar telescope [J]. *Proc. SPIE.* 2003: 406-413

[100] AZZAM R M A. Division-of-amplitude Photopolarimeter (DOAP) for the simultaneous measurement of all four Stokes parameters of light [J]. *J. Mod. Opt.*, 1982, **29**(5): 685-689

[101] MULLER D, MARSDEN R G, ST CYR O C, GILBERT H R. Solar Orbiter: exploring the Sun heliosphere connection [J]. *Solar Phys.*, 2013, **285**: 25-70

[102] SMITH E J, WENZEL K P, PAGE D E. Ulysses at Jupiter: an overview of the encounter [J]. *Science*, 1992, **257**: 1503

[103] SUN Z Z, ZHANG T X, ZHANG H, *et al.* The technical design and achievements of Chang'E-3 probe [J]. *Sci. Sin. Tech.*, 2014, **44**: 331-343

[104] Future out-of-ecliptic and in-situ observations of the Sun [R]//International Space Science Institute (ISSI) Annual Report 2010—2011. Bern: International Space Science Institute,2011

[105] Solar Probe Plus report of the Science and Technology Definition Team (STDT) [R]. Washington: NASA, 2008

[106] FOX N J, VELLI M C, BALE S D, *et al.* The Solar Probe Plus mission: Humanity's first visit to our star [J]. *Space Sci. Rev.*, 2015. DOI: 10.1007/s11214-015-0211-6

[107] MARSDEN R G, MULLER D. Solar Orbiter definition study report (Red Book). Paris: ESA, 2011

[108] KUZNETSOV V D, ORAEVSKY V N. Russian plans for solar and heliospheric physics [C]//Proceedings of a crossroads for European solar & heliospheric physics. Tenerife: ESA, 1998: 417

[109] ORAEVSKY V N, GALEEV A A, KUZNETSOV V D, ZELENYI L M. Russian payload for "interhelioprobe" ("interhelios") mission [J]. *Adv. Space Res.*, 2002, **29**: 2041

[110] MACDONALD M, ATZEI A, FALKNER P, *et al.* Solar polar orbiter: a solar sail technology reference study [J]. *J. Spacecraft Rockets*, 2006, **43**: 960-972

[111] APPOURCHAUX T, LIEWER P, WATT M, *et al.* POLAR investigation of the Sun POLARIS [J]. *Exp. Astron.*, 2009, **23**: 1079-1117

[112] LIU Z X. Geospace Double Star exploration project [J]. *Chin. J. Geophys.*, 2001, **44**(4): 573-580

[113] WU J, ZHU G W, ZHAO H, *et al.* Overview of scientific objects of China-Russia joint Mars exploration program YH-1 [J]. *Chin. J. Space Sci.*, 2009, **29**(5): 449-455